

FULL PAPER

Microwave-assisted biosynthesis of $C_{12}A_7$ nanopowders from *Aloe Vera* leaf extract

Waramon LANGLAR^{1,†}, Areeya AEIMBHU⁴, Pichet LIMSUWAN¹ and Chesta RUTTANAPUN^{1,2,3}

¹Department of Physics, Faculty of Science, King Mongkut's Institute of Technology Ladkrabang, Bangkok 10520, Thailand

²Smart Materials Research and Innovation Unit, Faculty of Science, King Mongkut's Institute of Technology Ladkrabang, Bangkok 10520, Thailand

³Thailand Center of Excellence in Physics, Ministry of Higher Education, Science, Research and Innovation, 328 Si Ayutthaya Road, Bangkok 10400, Thailand

⁴Department of Physics, Faculty of Science, Srinakharinwirot University, Bangkok 10110, Thailand

In this paper, the synthesis of $C_{12}A_7$ nanopowders with OH^- specie inside cage via biological method using *Aloe Vera* (*A. vera*) leaf extract with different concentrations of 0, 15, 20, 25 and 50%, and microwave-assisted synthesis was reported. The effects of *A. vera* leaf extract concentration on the structure, morphology and specific surface area of $C_{12}A_7$ nanopowders were characterized by X-ray diffraction (XRD), field emission scanning electron microscopy and N_2 gas adsorption-desorption isotherm, respectively. The functional groups of $C_{12}A_7$ nanopowders with OH^- specie inside cage were analyzed by fourier transform infrared spectroscopy (FT-IR). The XRD patterns showed that the pure peak of $C_{12}A_7$ was obtained from the samples prepared with *A. vera* leaf extract concentration of 20% and above. The minimum crystallite size of the $C_{12}A_7$ nanopowders was found to be 43.17 nm for the sample prepared with 25% *A. vera* leaf extract concentration. The maximum specific surface area (S_{BET}) obtained from N_2 gas adsorption-desorption isotherm was found to be 17.25 m²/g with a minimum pore size of 12.24 nm for the sample prepared with 25% *A. vera* leaf extract concentration. The FT-IR spectra of $C_{12}A_7$ prepared with *A. vera* leaf extract reveals the presence of amide of protein in *A. vera* leaf bonded to $C_{12}A_7$ indicating the biological responsibility for the synthesis of $C_{12}A_7$. Furthermore, in this work with the microwave-assisted synthesis of $C_{12}A_7$ nanopowders, the calcining time could be reduced by 10 h compared with a chemical process and temperature could be reduced to 900 °C compared with a standard sintering temperature.

©2020 The Ceramic Society of Japan. All rights reserved.

Key-words : $C_{12}A_7$, *A. vera* leaf extract, Biosynthesis, Microwave assisted

[Received August 13, 2019; Accepted February 19, 2020]

1. Introduction

The mayenite or $C_{12}A_7$ is binary compound of the calcia-alumina ($CaO-Al_2O_3$) with the chemical formula of $Ca_{12}Al_{14}O_{33}$. The $C_{12}A_7$ is a rare mineral of cubic symmetry, originally reported from the Eifel volcanic complex in Germany.¹⁾ It has the space group $I\bar{4}3d$ with $a = 1.198$ nm.²⁾ The chemical formula for the unit cell may be represented as $[Ca_{24}Al_{28}O_{64}]^{4+} + 2O^{2-}$, the former denotes a positively charged lattice framework with 12 cages, and the latter are called "free oxygen ions (O^{2-})".³⁾ The two free O^{2-} ions are entrapped as counter anions in the cage in the stoichiometric composition because of the cage diameter is larger by ~50% than the diameter of O^{2-} .⁴⁾ The free O^{2-} ions can be replaced by anions such as H^- ,³⁾ O^- ,^{5),6)} O_2^- ,⁷⁾ OH^- ,^{6),8)} Cl^- ,^{6),9)} F^- ,^{6),10)} CN^- ,^{6),11)} S^- , N^- ⁶⁾ and

e^- .^{12),13)} The contains of O^- and OH^- species in the cages are highly active with gas, benzene and water at the surface of the sample.¹⁴⁾ Especially, the OH^- specie can be produced via reaction: $O^-_{(surface)} + H_2O_{(surface)} \rightarrow OH^-_{(surface)} + OH_{(surface)}$ at temperature rising from 500 to 800 °C.¹⁴⁾

Various methods were used to prepare $C_{12}A_7$ in different forms such as single crystal, powder and thin film. $C_{12}A_7$ powders are generally prepared via a conventional solid state reaction using $CaCO_3$ and Al_2O_3 . The process took 4–24 h under sintering temperature between 1100–1350 °C.^{15)–18)} The long time sintering is necessary for the formation of $C_{12}A_7$ in solid state reaction because of poor homogeneity of the mixed starting powders.¹⁹⁾ For high sintering temperature in solid state reaction, it results in low specific surface area and large grain size. Therefore, the chemical synthesis have attracted attention to synthesize $C_{12}A_7$ due to the formation of single phase, low temperature synthesis, high specific surface area and small particle size.²⁰⁾ These chemical processes include

[†] Corresponding author: W. Langlar; E-mail: l.waramon@gmail.com

sol-gel and ball-milling method,²¹⁾ citrate sol-gel,²²⁾ modified glycine/nitrate procedure,²³⁾ oxalate precursor method²⁴⁾ have been used to produce $C_{12}A_7$ powders successfully.

In recent years, more articles related to green chemistry and biosynthesis method of materials have been published because of the use of nontoxic substances, cost-effective and eco-friendly process.²⁵⁾ Biosynthesis is a process using biological resource in nature such as plant extract, algae, fungi, bacteria and viruses^{26)–28)} for the synthesis of materials. Biosynthesis using biological molecules is derived from the plant sources in the form of extracts exhibiting superiority over the chemical method.²⁹⁾ Moreover, the plant extracts are benign, nontoxic, human health benefit, safe to handle and possess a broad variability of metabolites that may aid in reduction of metal compound into nanoparticles.³⁰⁾

The *Aloe vera* (*A. vera*) is a perennial, drought-resisting and succulent plant belonging to the Liliaceae family.³¹⁾ Most of *A. vera* plants are indigeneous to Africa, however, nowadays they have been widely distributed in the tropical and subtropical regions of the world. The *A. vera* leaf consists of three parts, each has chemical compound. The outer layer, the green rind or cuticle of the *A. vera* plant consists of multiple layers interspersed with chloroplasts.³²⁾ It has been reported to have a high proportion of α -cellulose and inferred to play a role in the synthesis of carbohydrates and proteins.³³⁾ The middle layer, the bitter yellow latex (exudate) contains anthraquinones and glycoside. The inner layer is composed of large thin walled parenchyma cells that store *A. vera* gel (mucilage).³²⁾ The *A. vera* gel consists of about 99.5% water and it has a pH of 4–5 with organic acid, mineral, polysaccharides, vitamin, and protein.^{31)–35)}

The *A. vera* is one of the most popular botanical plants used in medicine, dietary supplements and cosmetics due to its phytochemical contains such as alkaloid, saponins, tannins, sterols, terpenoids, carbohydrate, protein, glycoside, flavonoids and phenol.^{36)–38)} Phytochemical exhibits several important biological activities such as wound healing, antimicrobial, antidiabetic, anti-inflammatory.^{31),39),40)} Furthermore, they have played a role in synthesizing nanomaterials as these compounds can reduce and stabilize agents' responsible for the synthesis of nanostructure materials.⁴¹⁾ The *A. vera* leaf extracts have been widely used for the synthesis of (i) metal nanoparticles (NPs) such as $Ag^{42),43)}$ and $Au^{43),44)}$ etc.; (ii) metal oxide NPs such as TiO_2 ,⁴⁵⁾ In_2O_3 ,⁴⁶⁾ ZnO ³⁸⁾ and CuO ,⁴⁷⁾ and (iii) multi-element oxides such as $Co_xZn_{1-x}Al_2O_4$ nano-crystal⁴⁸⁾ and MFe_2O_4 ($M = Co, Cu, Mn, Mg, Ni, Zn$) nanocrystalline.^{49),50)}

A household and laboratory microwave ovens, which operate at 2.45 GHz and a wavelength of 12.2 cm was used in this experiment. Microwave ovens have been used in laboratory for nanostructure materials synthesis due to microwave heating is generated internally within the material, instead of originating from the external source.⁵¹⁾ Therefore, it can provide a higher heating rate and a more

homogeneous heating,⁵²⁾ leading to a more homogeneous nucleation and a shorter crystallization time.⁵³⁾

In this paper, we report on the synthesis of $C_{12}A_7$ nanoparticles which contain OH^- specie in cage via biological method using *A. vera* leaf extract and microwave-assisted synthesis. The effects of *A. vera* leaf extract concentration as bioreducing or complexing agent on morphology, surface area and structure of $C_{12}A_7$ were investigated.

2. Experimental procedure

2.1 Materials

All chemical materials were analytical graded and purchased from various commercial sources. Aluminium tri-sec-butoxide $\{Al[OCH(CH_3)C_2H_5]_3; ATSB\}$ and ethyl acetoacetate ($CH_3COCH_2COOC_2H_5$; ETAC) were from Acros, calcium nitrate tetrahydrate $[Ca(NO_3)_2 \cdot 4H_2O]$ and absolute ethanol was from Carlo Ebra.

2.2 Preparation of *A. vera* leaf extract

A. vera extract was prepared by taking about 50 g of gel from *A. vera* leaf. It was blended and added with boiled deionized water. The mixture was heated on the hot plate at 90 °C for 1 h and cooled down to room temperature. *A. vera* extract was obtained from the filtered gel and stored at a temperature of 4 °C.

2.3 Synthesis of $C_{12}A_7$ powders

The ATSB and $Ca(NO_3)_2 \cdot 4H_2O$ were used as starting materials. The ATSB and $Ca(NO_3)_2 \cdot 4H_2O$ were added into ETAC with a molar ratio of 12:14:12 and stirred at room temperature for 30 min. Then, the 20.88 ml of absolute ethanol was dropped into 37.78 g of the mixture and stirred vigorously at room temperature for 30 min. Each mixture was added with four different concentrations of *A. vera* leaf extract of 15, 20, 25 and 50% and stirred vigorously for 30 min. The solutions should become white and clear. All samples mixed with *A. vera* leaf extract and a sample without *A. vera* leaf extract were sonicated by an ultrasonic cleaner for 5 h to reduce particle size. It was found that only the sample without *A. vera* leaf extract became the form of gel. However, the samples with *A. vera* leaf extract are in the form of white colloidal solution. All samples were then heated in an electric oven at 90 °C for 8 h. The yellow-brown gel was formed except for the sample without *A. vera* leaf extract which became white liked-cake gel. The gels were grinded and heated in a domestic microwave oven (Samsung, ME711K/XST) at a power of 450 W for 30 min at temperature around 100 °C. OH^- functional group¹⁴⁾ was maintained to prepare for nano precursor and calcine temperature was lower down to prepare for $C_{12}A_7$ nanopowders. The white powder was obtained and then it was calcined in an electric furnace under ambient condition at 900 °C for 3 h for forming phase of $C_{12}A_7$ with OH^- specie in the cage in order to react with $O_{(surface)}^-$ and OH^- functional groups at temperature rising from 500 to 800 °C.¹⁴⁾ Finally, the white fine-powders of $C_{12}A_7$ were obtained as $C_{12}A_7$ nanopowders with OH^- inside the cage.

2.4 Characterization

The structure of C₁₂A₇ powders were characterized by X-ray diffraction (XRD; PANalytical, Empyrean) using Cu K α radiation operated at 40 kV and 40 mA. The XRD patterns were recorded in the 2 θ range of 15 to 65° with a scanning rate of 2°/min. The morphology of C₁₂A₇ powders was investigated using field emission scanning electron microscopy (FE-SEM; JEOL 6301F) with energy dispersive X-ray analysis (EDX). The specific surface area (S_{BET}) was measured by Brunauer–Emmett–Teller (BET) analysis using N₂ gas adsorption–desorption technique at –196 °C on micromeritics (TriStar II 3020). Cumulative pore volume and average pore size were calculated by Barret-Joyner-Halenda (BJH) from adsorption isotherm. The functional groups of materials were analyzed by fourier transform infrared spectroscopy (FT-IR) spectroscopy on Thermo Scientific (Nicolet 6700) with collected data in the range of 400–4000 cm^{–1}.

3. Results and discussion

3.1 XRD result

The XRD patterns of C₁₂A₇ powders synthesized via biological method with different *A. vera* leaf extract concentrations of 0, 15, 20, 25 and 50% are shown in **Fig. 1**. Reference peaks of C₁₂A₇ were marked according to JCPDS file number 09-0413. For C₁₂A₇ powder with 0% *A. vera* leaf extract concentration, the peaks of CaAl₂O₄ (CA), Ca₅Al₆O₁₄ (C₅A₃), Ca₃Al₂O₆ (C₃A) and Ca₁₂Al₁₄O₃₃ (C₁₂A₇) were observed. For C₁₂A₇ prepared with different

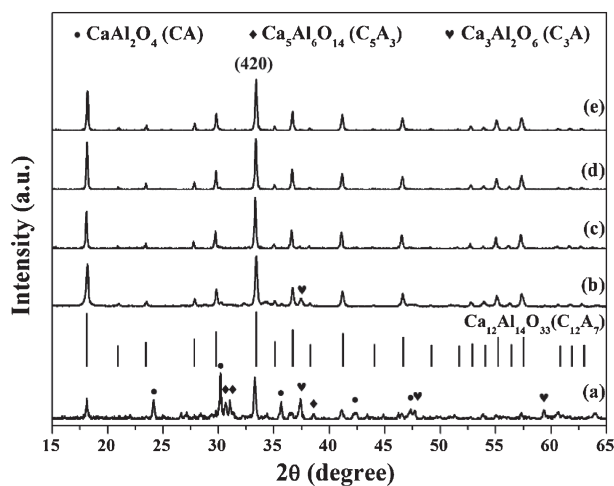


Fig. 1. XRD patterns of C₁₂A₇ powders synthesized via biological method with different *A. vera* leaf extract concentrations of: (a) 0, (b) 15, (c) 20, (d) 25 and (e) 50%.

A. vera leaf extract concentrations, major peaks of C₁₂A₇ were observed. At 15% *A. vera* leaf extract concentration, a small peak of C₃A can be seen. Further increase the *A. vera* leaf extract concentration from 20 to 50%, all peaks of CA, C₅A₃ and C₃A disappeared except for the peaks of C₁₂A₇. The crystalline size (*D*) were determined by Scherrer equation:

$$D = \frac{0.9\lambda}{\beta \cos \theta} \quad (1)$$

where *D* is crystallite size (nm), λ is the wavelength of X-ray (Cu K α), β is the full width at half maximum and θ corresponds to the peak position. The obtained crystalline sizes are given in **Table 1**. It was observed that the crystallite size decreased as the *A. vera* leaf extract concentration increased. In general, the crystallite size for all powders was less than 100 nm and the smallest crystallite size was found as 43.17 nm for 25% *A. vera* leaf extract concentration. These results were based on C₁₂A₇ powders that are nanopowders for all samples prepared with different *A. vera* leaf extract concentrations.

Meanwhile, the lattice constant (*a*) of the cubic C₁₂A₇ nanopowders which correspond to (420) plane prepared with different *A. vera* leaf extract concentrations of 0, 15, 20, 25 and 50% were determined and found to be 12.032, 12.014, 11.992, 11.991 and 11.981 Å, respectively as shown in Table 1. The lattice constant was slightly decreased as the *A. vera* leaf extract concentration increased. The value of the lattice constants obtained in this work matched perfectly with the previous report.²⁾

3.2 FE-SEM

Figure 2 shows the FE-SEM morphology images of C₁₂A₇ powders prepared with different *A. vera* leaf extract concentrations of 0, 15, 20, 25 and 50%. The particle size was determined by Image J program and the results are shown in Table 1. The particle size decreased as the *A. vera* leaf extract concentration increased from 0 to 25%. However, further increased to the *A. vera* leaf extract concentration up to 50%, the particle size increased. The largest particle size of 72 nm was observed for 0% *A. vera* leaf extract concentration. This can be explained by the morphology as shown in Fig. 2(a). The particles agglomerated and formed irregular particles shape with large particle size. In Figs. 2(b)–2(d), as *A. vera* leaf extract concentration was increased from 15 to 25%, the porosity of C₁₂A₇ powder increased, which resulted to the decreased of particle size. The increase in porosity with increase *A. vera* leaf extract concentrations from 15 to

Table 1. Effects of *A. vera* leaf extract concentration on structure and morphology of C₁₂A₇

<i>A. vera</i> leaf extract concentration (%)	Crystallite size (nm)	<i>a</i> (Å)	Particle size (nm)	Surface area (m ² /g)	Cumulative pore volume (BJH; cm ³ /g)	Average pore size (BJH; nm)
0	53.33	12.032	72	2.69	0.010	21.67
15	45.64	12.014	64	5.60	0.018	16.83
20	44.57	11.992	54	6.09	0.019	16.40
25	43.17	11.991	51	17.25	0.021	12.24
50	48.98	11.981	67	5.50	0.016	15.82

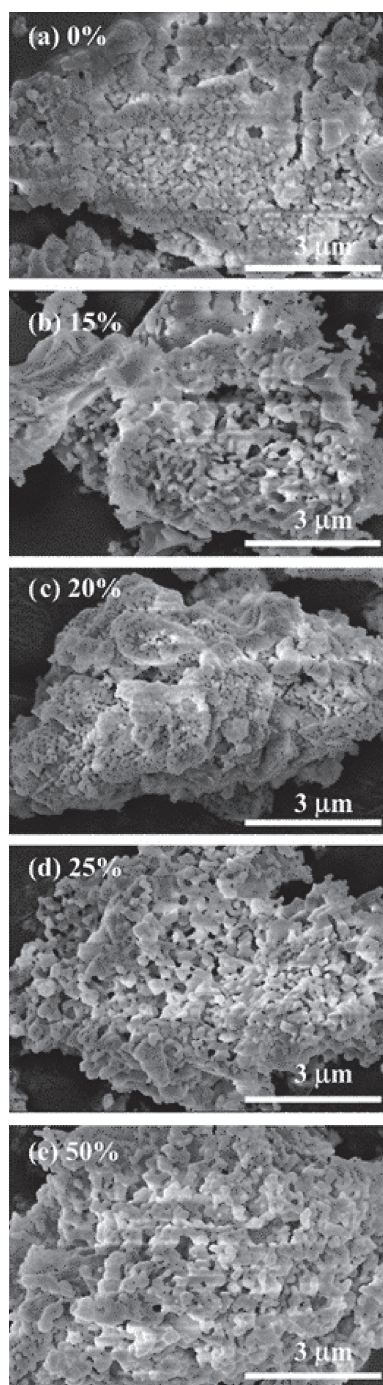


Fig. 2. FE-SEM images show the morphology of $C_{12}A_7$ powders prepared with different *A. vera* leaf extract concentrations of: (a) 0, (b) 15, (c) 20, (d) 25 and (e) 50%.

25% can be confirmed by BET analysis results. When the *A. vera* leaf extract concentration was increased from 25 to 50%, the particle size increased with a loss porosity of $C_{12}A_7$ as shown in Figs. 2(d) and 2(e). The increase of porosity may be due to the occurrence of the high volume of released gas⁵⁴⁾ such as N_2 , O_2 , CO_2 and H_2O during the synthesis by microwave.

Figure 3 shows the EDX analysis of $C_{12}A_7$ nanopowders. They consisted of Ca, O and Al peaks which confirm that there were no impurities in the sample.

3.3 N_2 gas adsorption–desorption isotherm

Nitrogen adsorption–desorption isotherm can be displayed in graphical form with amount of gas adsorbed (cm^3/g) against relative pressure (P/P_0) in the range of 0.01 to 0.99 P/P_0 . The nitrogen adsorption–desorption isotherm curves of all samples were similar and correspond to the type IV according to the IUPAC, which was associated with capillary condensation taking place in mesoporous structure.⁵⁴⁾ **Figure 4(a)** shows a typical adsorption–desorption isotherm curve for $C_{12}A_7$ prepared with 25% of *A. vera* leaf extract concentration with reaction between $OH^-_{(surface)}$ and N_2 gas at surface.¹⁴⁾ The OH^- species played a key role in the reaction with the N_2 gas at surface. The type of hysteresis loop appeared on isotherm curve was H3-type hysteresis, which indicated the agglomeration of plate-like particles giving rise to the slit-shape pore.^{55),56)}

Figure 4(b) shows the adsorption isotherm curves for $C_{12}A_7$ prepared with different *A. vera* leaf extract concentrations. The adsorption isotherm in Fig. 4(b) at low relative pressure ($0.05 < P/P_0 < 0.35$) associated with a monolayer adsorption. Then, the BET surface area was obtained from monolayer adsorption volume using BET method. The $C_{12}A_7$ prepared with 25% *A. vera* leaf extract concentration has higher adsorption volume of nitrogen than other concentrations. The results on surface area (S_{BET}) obtained from BET method are given in Table 1. $C_{12}A_7$ with 0% *A. vera* leaf extract concentration has a surface area of $2.69 m^2/g$ which corresponded to the transformation of sol to gel. Histograms in Fig. 4(c) present $C_{12}A_7$ with *A. vera* leaf extract concentration from 15 to 50% where the precipitation occurred with surface areas 5.60 , 6.09 , 17.25 and $5.50 m^2/g$, respectively. The results showed that $C_{12}A_7$ with 25% *A. vera* leaf extract concentration has the highest surface area ($17.25 m^2/g$) among the samples. This was due to a large amount of gases released⁵⁴⁾ during the thermal decomposition of powder precipitation. The results also showed the surface area of $C_{12}A_7$ with 50% *A. vera* leaf extract concentration decreased to $5.50 m^2/g$. It may be due to the incomplete combustion reaction of released gas⁵⁷⁾ in the microwave-assisted synthesis. The results on the surface area of $C_{12}A_7$ obtained in this work can be further used for catalysis application.

The pore volume and the pore size were calculated by BJH method. The results on pore volume and pore size of $C_{12}A_7$ with different *A. vera* leaf extract concentrations of 0, 15, 20, 25 and 50% are given in Table 1. The high adsorption volume corresponding to high pore volume led to high surface area as shown in Table 1.

3.4 FT-IR spectroscopy

FT-IR spectra of *A. vera* leaf extract, $C_{12}A_7$ powder and $C_{12}A_7$ prepared with 25% *A. vera* leaf extract concentration and $C_{12}A_7$ powders are shown in **Fig. 5**.

As shown in Fig. 5(a), the FT-IR spectra of *A. vera* leaf extract exhibited a broad band between the range of 3450 – $3250 cm^{-1}$ with a peak at $3350.27 cm^{-1}$. This was due to $-OH$ group in alcohol and phenol.⁵⁸⁾ The peaks at 1641.11

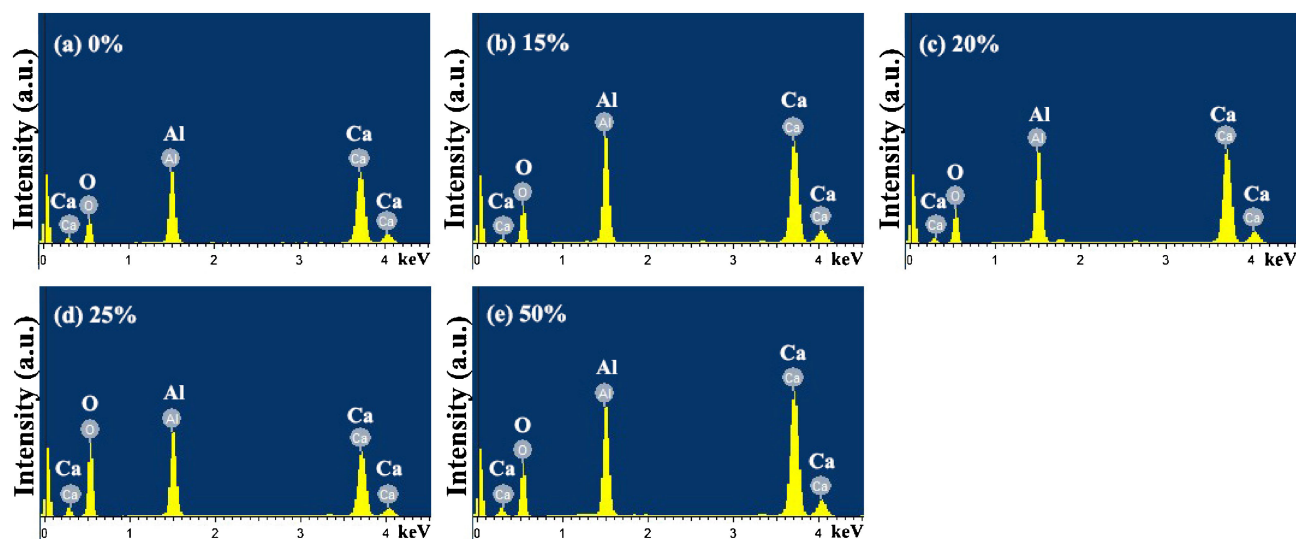


Fig. 3. EDX analysis of $C_{12}A_7$ powders prepared with different *A. vera* leaf extract concentrations of: (a) 0, (b) 15, (c) 20, (d) 25 and (e) 50%.

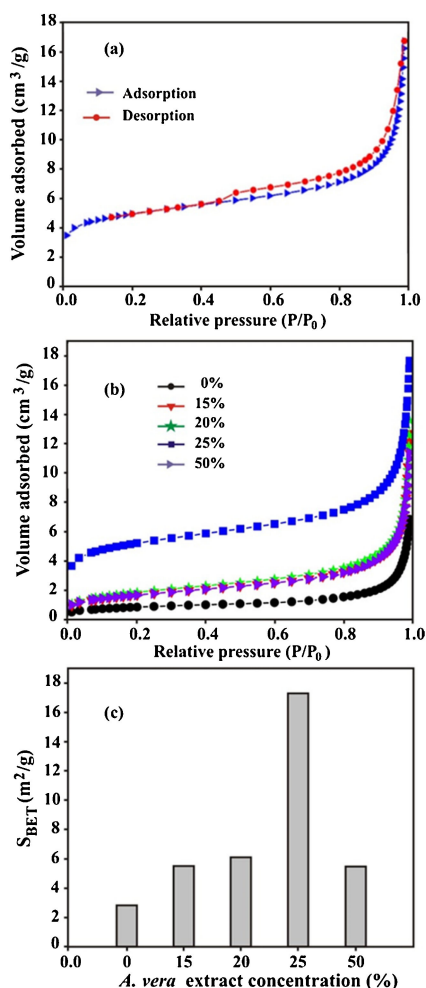


Fig. 4. (a) Nitrogen adsorption-desorption isotherm of $C_{12}A_7$ nanopowder prepared with 25% *A. vera* leaf extract concentrations, (b) Nitrogen adsorption isotherm and (c) Histogram S_{BET} of $C_{12}A_7$ nanopowder prepared with different concentrations of *A. vera* leaf extra.

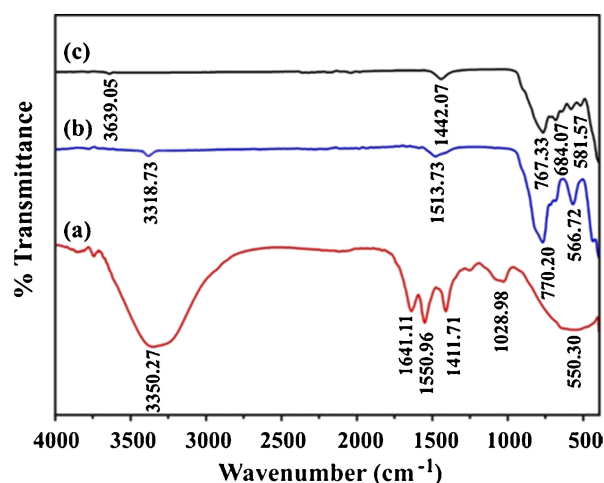


Fig. 5. FT-IR spectra of: (a) *A. vera* leaf extract, (b) $C_{12}A_7$ with 25% *A. vera* leaf extract concentration and (c) $C_{12}A_7$ powder.

and 1550.96 cm^{-1} indicated the presence of amide I and II band of protein^{59)–61)} in *A. vera* leaf extract, while the peak at 1411.71 cm^{-1} was assigned to the aromatic frame stretching vibration.⁶²⁾ The peak at 1028.98 cm^{-1} of aromatic was assigned to C–O–C functional group of polysaccharide.^{61),63)} The result of FT-IR spectra of *A. vera* leaf extract revealed the presence of functional group such as alcohol, phenol, amide of protein, aromatic and C–O–C of polysaccharide.

As can be seen from FT-IR spectra of $C_{12}A_7$ powder in Fig. 5(c), the peak at 3639.05 cm^{-1} was assigned to the –OH group indicated the –OH group bonded to aluminum and calcium ($Al/Ca\text{--}OH$),⁶⁴⁾ while 1442.07 cm^{-1} peak was assigned to CH_2 group. Three peaks at 767.33 , 684.07 and 581.57 cm^{-1} were due to the Al–O vibration. The peaks at 767.33 and 684.07 cm^{-1} were related to AlO_4 tetrahedral and the AlO_6 octahedral at 581.57 cm^{-1} .⁶⁵⁾

In the case of $C_{12}A_7$ prepared with 25% *A. vera* leaf extract as shown in Fig. 5(b), the peaks at 3318.73 ,

1513.73, 770.20 and 566.72 cm^{-1} were observed. The peak at 3318.73 cm^{-1} was due to Al/Ca bonded to the -OH group in phenol¹⁴⁾ and alcohol while 1513.73 cm^{-1} peak was assigned to amide II band of protein, indicated the organic compound of *A. vera* leaf extract bonded to C_{12}A_7 . Two peaks at 770.20 and 566.72 cm^{-1} indicated the Al-O bond. The OH^- specie inside cages was produced from the reaction of O^- and OH functional group (which exists in dry powder precursor resulting from ATSB, ETAC and *A. vera* leaf at microwave process) in calcine process at temperature rising from 500 to 800 $^{\circ}\text{C}$.

The biological molecule of *A. vera* leaf extract may act as bioreducing or complexing agent. The phenol and protein present in *A. vera* leaf extract were responsible for the reduction of metal ion.⁴¹⁾ While, the phenol and protein in *A. vera* leaf extract may behave as complexing agent where the complexing agent chelate metal ion in solution and homogeneously mixed in atomic scale.⁴⁹⁾ The concentration of *A. vera* leaf extract can affect C_{12}A_7 nanopowder structure with the OH^- specie in the cages as shown in Table 1 and Fig. 5.

4. Conclusions

The C_{12}A_7 nanopowders with the OH^- specie in the cages have been successfully synthesized via biological method using *A. vera* leaf extract of different concentrations of 0, 15, 20, 25 and 50%, and microwave-assisted synthesis. The effects of *A. vera* leaf extract concentration on the structure, morphology and specific surface area of C_{12}A_7 nanopowders with the OH^- specie in the cages were investigated by XRD, FE-SEM and N_2 gas adsorption-desorption isotherm. In addition, the functional groups of C_{12}A_7 nanopowders with the OH^- specie in the cages were analyzed by FT-IR. The XRD and BET surface area results showed that the C_{12}A_7 nanopowders prepared with 25% *A. vera* leaf extract concentration has a minimum crystallite size of 43.17 nm with a maximum BET surface area of 17.25 m^2/g and a minimum pore size of 12.24 nm. It can be concluded that the optimum concentration of *A. vera* leaf extract to be added in the synthesis of C_{12}A_7 is 25%.

Acknowledgments Authors would like to thank the Faculty of Science, King Mongkut's Institute of Technology Ladkrabang (KMUTL) for supporting facilities. This work was supported by the Srinakharinwirot University (Grant No. 086/2563).

Reference

- 1) R. C. Ropp, "Encyclopedia of The Alkaline Earth Compounds", Ed. by R. C. Ropp Elsevier, Amsterdam (2013) pp. 481-635.
- 2) E. V. Galuskin, J. Kusz, T. Armbruster, R. Bailau, I. O. Galuskin, B. Ternes and M. Murashko, *Mineral. Mag.*, **76**, 707-716 (2012).
- 3) K. Hayashi, S. Matsuishi, T. Kamiya, M. Hirano and H. Hosono, *Nature*, **419**, 462-465 (2002).
- 4) H. Hosono, "Handbook of Advanced Ceramics Materials Application Processing and Properties", Ed. by S. Somiya Elsevier, USA (2013) pp. 455-487.
- 5) K. Hayashi, M. Hirano, S. Matsuishi and H. Hosono, *J. Am. Chem. Soc.*, **124**, 738-739 (2002).
- 6) J. P. Eufinger, A. Schmidt, M. Lerch and J. Janek, *Phys. Chem. Chem. Phys.*, **17**, 6844-6857 (2015).
- 7) K. Hayashi, S. Matsuishi, N. Ueda, M. Hirano and H. Hosono, *Chem. Mater.*, **15**, 1851-1854 (2003).
- 8) J. Li, F. Huang, L. Wang, S. Q. Yu, Y. Torimoto, M. Sadakata and Q. X. Li, *Chem. Mater.*, **17**, 2771-2774 (2005).
- 9) J. Q. Sun, L. Gong, J. Shen, Z. Lin and Q. X. Li, *Acta Phys.-Chim. Sin.*, **26**, 795-798 (2010).
- 10) C. Song, J. Sun, J. Li, S. Ning, M. Yamamoto, J. Tu, Y. Torimoto and Q. Li, *J. Phys. Chem. C*, **112**, 19061-19068 (2008).
- 11) A. Schmidt, M. Lerch, J. P. Eufinger, J. Janek, R. Dolle, H. D. Wiemhofer, I. Tranca, M. M. Islam, T. Bredow, H. Boysen and M. Hoelzel, *Solid State Sci.*, **38**, 69-78 (2014).
- 12) S. Matsuishi, Y. Toda, M. Miyakawa, K. Hayashi, T. Kamiya, M. Hirano, I. Tanaka and H. Hosono, *Science*, **301**, 626-629 (2003).
- 13) S. W. Kim, S. Matsuishi, T. Nomura, Y. Kubota, M. Takata, K. Hayashi, T. Kamiya, M. Hirano and H. Hosono, *Nano Lett.*, **7**, 1138-1143 (2007).
- 14) T. Dong, Z. Wang, T. Kan and Q. Li, *Chin. J. Chem. Phys.*, **20**, 297-304 (2007).
- 15) B. Raab and H. Poellmann, *Thermochim. Acta*, **513**, 106-111 (2011).
- 16) S. Watauchi, I. Tanaka, K. Hayashi, M. Hirano and H. Hosono, *J. Cryst. Growth*, **237-239**, 801-805 (2002).
- 17) S. G. Yoon, S. W. Kim, M. Hirano, D. H. Yoon and H. Hosono, *Cryst. Growth Des.*, **8**, 1271-1275 (2008).
- 18) M. Ruzsak, S. Witkowski, P. Pietrzyk, A. Kotarba and Z. Sojka, *Funct. Mater. Lett.*, **4**, 183-186 (2011).
- 19) M. Matsuda, Y. Inda, W. Hisamatsu, K. Yamashita and T. Umegaki, *J. Mater. Sci. Lett.*, **15**, 933-934 (1996).
- 20) M. A. Gulgun, O. O. Popoola and W. M. Kriven, *J. Am. Ceram. Soc.*, **77**, 531-539 (1994).
- 21) K. Ozawa, N. Sakamoto, N. Wakiya and H. Suzuki, *J. Ceram. Soc. Jpn.*, **119**, 460-463 (2011).
- 22) S. N. Ude, C. J. Rawn, R. A. Peascoe, M. J. Kirkham, G. L. Jones and E. A. Payzant, *Ceram. Int.*, **40**, 1117-1123 (2014).
- 23) B. Matovic, M. Prekajski, J. Pantic, T. Brauniger, M. Rosic, D. Zagorac and D. Milivojevic, *J. Eur. Ceram. Soc.*, **36**, 4237-4241 (2016).
- 24) M. M. Rashad, A. G. Mostafa and D. A. Rayan, *J. Mater. Sci.-Mater. El.*, **27**, 2614-2623 (2015).
- 25) K. B. Narayanan and N. Sakthivel, *Adv. Colloid Interfac.*, **169**, 59-79 (2011).
- 26) K. N. Thakkar, S. S. Mhatre and R. Y. Parikh, *Nanomed-Nanotechnol.*, **6**, 257-262 (2010).
- 27) L. Castro, M. L. Blazquez, J. A. Munoz, F. Gonzalez and A. Ballester, *Rev. Adv. Sci. Eng.*, **3**, 1-18 (2014).
- 28) P. Velusamy, G. V. Kumar, V. Jeyanthi, J. Das and R. Pachaiappan, *Toxicol. Res.*, **32**, 95-102 (2016).
- 29) S. Ahmed, M. Ahmad, B. L. Swami and S. Ikram, *J. Adv. Res.*, **7**, 17-28 (2016).
- 30) K. K. Yadav, J. K. Singh, N. Gupta and V. Kumar, *J. Mater. Environ. Sci.*, **8**, 740-757 (2017).
- 31) P. Liu, D. Chen and J. Shi, *Asian J. Chem.*, **25**, 6477-6485 (2013).
- 32) M. D. Boudreau and F. A. Beland, *J. Environ. Sci. Heal.*

- C., 24, 103–154 (2006).
- 33) A. Balaji, M. V. Vellayappan, A. A. John, A. P. Subramanian, S. K. Jaganathan, M. S. Kumar, A. A. M. Faudzi, E. Supriyanto and M. Yusof, *RSC Adv.*, 5, 86199–86213 (2015).
 - 34) S. Rahman, P. Carter and N. Bhattarai, *J. Funct. Biomater.*, 8, 1–17 (2017).
 - 35) J. H. Hamman, *Molecules*, 13, 1599–1616 (2008).
 - 36) D. K. Patel, K. Patel and S. P. Dhanabal, *J. Acute Dis.*, 1, 47–50 (2012).
 - 37) E. Raphael, *GARJEST.*, 1, 014–017 (2012).
 - 38) D. Mahendiran, G. Subash, D. A. Selvan, D. Rehana, R. S. Kumar and A. K. Rahiman, *Bio. Nano. Sci.*, 7, 530–545 (2017).
 - 39) F. Habeeb, E. Shakir, F. Bradbury, P. Cameron, M. R. Taravati, A. J. Drummond, A. I. Gray and V. A. Ferro, *Methods*, 42, 315–320 (2007).
 - 40) M. M. Sharif and V. Sandeep, *Int. J. Biol. Med. Res.*, 2, 466–471 (2011).
 - 41) P. Dauthal and M. Mukhopadhyay, *Ind. Eng. Chem. Res.*, 55, 9557–9577 (2016).
 - 42) S. Medda, A. Hajra, U. Dey, P. Bose and N. K. Mondal, *Appl. Nanosci.*, 5, 875–880 (2015).
 - 43) S. P. Chandran, M. Chaudhary, R. Pasricha, A. Ahmad and M. Sastri, *Biotechnol. Progr.*, 22, 577–583 (2006).
 - 44) B. D. Sawle, B. Salimath, R. Deshpande, M. D. Bedre, B. K. Prabhakar and A. Venkataraman, *Sci. Technol. Adv. Mater.*, 9, 035012–035017 (2008).
 - 45) K. S. Venkatesh, S. R. Krishnamoorthi, N. S. Palani, V. Thirumal, S. P. Jose, F. M. Wang and R. Ilangovan, *Indian J. Phys.*, 89, 445–452 (2015).
 - 46) S. Maensiri, P. Laokul, J. Klinkaewnarong, S. Phokha, V. Promarak and S. Seraphin, *J. Optoelectron. Adv. Mater.*, 10, 161–165 (2008).
 - 47) P. P. N. Vijay Kumar, U. Shameem, P. Kollu, R. L. Kalyani and S. V. N. Pammi, *Bio. Nano. Sci.*, 5, 135–139 (2015).
 - 48) A. Manikandan, M. Durka, M. A. Selvi, S. A. Antony and J. Nanosci, *Nanotechno.*, 16, 357–373 (2016).
 - 49) S. Phumying, S. Labuayai, E. Swatsitang, V. Amornkitbamrung and S. Maensiri, *Mater. Res. Bull.*, 48, 2060–2065 (2013).
 - 50) P. Laokul, V. Amornkitbamrung, S. Seraphin and S. Maensiri, *Curr. Appl. Phys.*, 11, 101–108 (2011).
 - 51) G. Ramesh, R. V. Mangalaraja, S. Ananthakumar and P. Manohar, *Int. J. Phys. Sci.*, 8, 1729–1737 (2013).
 - 52) S. Boldrini, C. Mortalo, S. Fasolin, F. Agresti, L. Doubova, M. Fabrizio and S. Barison, *Fuel Cells*, 12, 54–60 (2012).
 - 53) A. Manikandan, R. Sridhar, S. Arul Antony and S. Ramakrishna, *J. Mol. Struct.*, 1076, 188–200 (2014).
 - 54) M. Radpour, S. M. Masoudpanah and S. Alamolhoda, *Ceram. Int.*, 43, 14756–14762 (2017).
 - 55) K. S. W. Sing, *Pure Appl. Chem.*, 57, 603–619 (1985).
 - 56) G. Leofanti, M. Padovan, G. Tozzola and B. Venturelli, *Catal. Today*, 41, 207–219 (1998).
 - 57) B. Pourgolmohammad, S. M. Masoudpanah and M. R. Aboutalebi, *Ceram. Int.*, 43, 3797–3803 (2017).
 - 58) J. A. D. Angelo and E. L. Zodrow, *Org. Geochem.*, 42, 1039–1054 (2011).
 - 59) A. Barth, *Biochim. Biophys. Acta.*, 1767, 1073–1101 (2007).
 - 60) M. Baldassarre, C. Li, N. Erimena, E. Goormaghtigh and A. Barth, *Molecules*, 20, 12599–12662 (2015).
 - 61) D. Y. Duygu, A. U. Udoh, T. B. Ozer, A. Akbulut, I. A. Erkaya, K. Yildiz and D. Guler, *Afr. J. Biotechnol.*, 11, 3817–3824 (2012).
 - 62) L. Ping, F. Gambier, A. Pizzi, Z. D. Guo and N. Brosse, *Cellul. Chem. Technol.*, 46, 457–462 (2012).
 - 63) S. Li, Y. Shen, A. Xie, X. Yu, X. Zhang, L. Yang and C. Li, *Nanotechnology*, 18, 405101 (2007).
 - 64) B. Stumpe, T. Engel, B. Steinweg and B. Marschner, *Environ. Sci. Technol.*, 46, 3964–3972 (2012).
 - 65) P. Tarte, *Spectrochim. Acta A*, 23A, 2127–2143 (1967).